ADVANCED MATERIALS INTERFACES
www.advmatinterfaces.de

Self-Assembled Nanostructured Photonic-Plasmonic Metasurfaces for High-Resolution Optical Thermometry

Giorgio Baraldi, Marina García Pardo, José Gonzalo, Rosalia Serna, and Johann Toudert**

Sensing devices for environment, safety, healthcare, and optoelectronic applications require an accurate and noninvasive monitoring of their temperature, because its variations markedly affect the overall response of the device. Monitoring the optical response of temperature-sensitive integrated photonic elements, such as microresonators or microinterferometers, is an appealing solution in this context. However, achieving high-resolution optical thermometry with such elements is unpractical and costly as this requires lithography processing, highly monochromatic laser sources, complex light coupling strategies. Here, a photonic-plasmonic metasurface design that enables practical optical thermometry with a sub-10^{-3} °C resolution is proposed. It is based on a self-assembled nanostructured material implemented with a lithography-free process. The optical response of the temperature-sensitive metasurface is probed using a white light source and by monitoring the optical phase in a standard reflectance configuration. This facile, yet powerful, sensing scheme stands on the effective response of the metasurface, which involves the hybridization of thin film interference and low-quality-factor plasmon resonances to enable a quasi-darkness response with a sharp spectral variation (jump) of the optical phase. Such jump is equivalent with a high-quality-factor resonator that yields a high sensor responsivity and thus enables high-resolution optical thermometry.

Optical monitoring is a powerful diagnostic and control tool needed for remote and noninvasive sensing applications in the environment, safety, healthcare, or optoelectronics areas. For such applications that aim at detecting low levels of gases, particles, biomolecules, or light, it is first primordial to monitor accurately temperature because its variations affect the overall response of the sensing device. Therefore, it will be desirable for the next generation of such devices to integrate, in microscale or smaller dimensions, high-resolution optical thermometry functionalities, i.e., the capability of monitoring with light very slight changes in their temperature.

In this context, monitoring the optical response of temperature-sensitive integrated photonic elements, such as microresonators[1–8] or microinterferometers[9,10] has arisen as an appealing solution. With such elements, temperature monitoring requires tracking the wavelength variation of narrow, high-quality-factor resonances (spectral width at the picometer scale). The reported responsivities reaching up to 200 pm per °C[7–10] indicate a higher resolution than other implementations, such as localized surface plasmon resonators,[11,12] surface plasmon polariton resonators,[13–15] Bragg gratings,[16] or Tamm structures.[17] Yet, although record resolutions down to the 10^{-9} °C range[6] have been obtained with microresonators, the reported responsivities imply that achieving even a 10^{-3} °C resolution requires a picometer precision in the determination of the resonance wavelength. Reaching such precision requires specific devices, such as highly monochromatic lasers as light source or bulky optoelectronic devices for signal processing. Furthermore, microresonators and microinterferometers suffer from their weak interaction with the incident light. Therefore, their use requires employing high optical powers or designing additional and specific in-coupling structures. The fabrication of such structures together with the microresonators and microinterferometers require high-accuracy lithography setups. In sum, although such photonic elements permit record high-resolution optical thermometry, they remain an unpractical and costly solution.

A promising and yet unexplored alternative for practical and cost-effective high-resolution optical thermometry consists in monitoring the optical response of temperature-sensitive metasurfaces. Metasurfaces[18–20] can support a rich variety of optical modes that enable a straightforward strong coupling of light in their subwavelength thickness. Furthermore, their optical response can be made broadly tunable through changes in their environment, enabling a dynamic shaping of the amplitude and phase of light.[21–35] Such tunability also opens the way to using metasurfaces as "wireless" sensors allowing an optical monitoring of their environment. Sensing with particularly

Dr. G. Baraldi, M. García Pardo, Dr. J. Gonzalo, Prof. R. Serna, Dr. J. Toudert
Laser Processing Group
Instituto de Óptica, IO
CSIC
Madrid 28006, Spain
E-mail: rosalia.serna@csic.es; johann.toudert@gmail.com

The ORCID identification number(s) for the author(s) of this article can be found under https://doi.org/10.1002/admi.201800241.

DOI: 10.1002/admi.201800241

high resolution has been demonstrated by monitoring the environment-sensitive optical response of metasurfaces presenting topological darkness.[36,37] Topological darkness is characterized by a zero amplitude and a phase singularity for the Fresnel reflection coefficient of the metasurface occurring at specific photon energies and angles of incidence. Although initially shown for linearly p-polarized light, topological darkness can also occur with other polarization states.[37–40] By slightly detuning the angle of incidence from topological darkness conditions, a small fraction of light is reflected by the metasurface and the phase of this light varies abruptly (or "jumps") with photon energy while remaining defined. In the spectral region of this jump, the reflected light phase is by far more sensitive to any change in the optical response of the environment-sensitive metasurface than the reflected light intensity. For this reason, monitoring the phase of light reflected by metasurfaces in quasi-darkness conditions enabled sensing with a particularly high resolution. This was successfully applied for the optical detection of very low levels of hydrogen and biomarkers using plasmonic metasurfaces as sensing platform.[36,37] Following a similar scheme, recent works have reported a high-resolution sensing potential for other material architectures such as 3D metamaterials,[40–42] surface plasmon polariton resonators,[43] or Tamm plasmonic structures.[44]

Here, we report a temperature-sensitive metasurface that enables practical high-resolution optical thermometry, based on the monitoring of its reflected light phase in quasi-darkness conditions. Such metasurface, which consists of a self-assembled photonic-plasmonic structure, enables a temperature resolution below the 10^{-3} °C range using a standard optical reflectance measurement configuration and a white light source. This facile and yet powerful experimental scheme for sensing is enabled by the effective response of the metasurface that involves the hybridization of thin film interference ("photonic") and low-quality-factor plasmon resonances ("plasmonic"), which together in the quasi-darkness conditions behave, in the optical phase space, like a high-quality-factor resonator that enables a high sensing resolution. These results show the potential of self-assembled photonic-plasmonic metasurfaces as a practical alternative to microresonators and microinterferometers for temperature sensing. Such class of metasurface can be fabricated without expensive lithography tools and enables a high resolution in easy-to-implement and cost-effective optical measurement conditions.

Nanostructured metasurfaces were fabricated by pulsed laser deposition. A silver (Ag) coating was first deposited on silicon substrates covered with a thin layer of amorphous aluminum oxide (a-Al_2O_3). Then this coating was annealed at 350 °C to form a well-defined 2D array of self-assembled Ag nanoparticles. Finally, an a-Al_2O_3 cover layer was deposited onto the Ag nanoparticles. **Figure 1**a depicts the metasurface structure before and after deposition of this cover layer ("uncover" and "cover," respectively). The "uncover" metasurface consists of an amorphous 2D array of Ag nanoparticles with a hemispherical shape and an average in-plane diameter near 100 nm. The top surface of these nanoparticles is in contact with air. In the "cover" metasurface, the Ag nanoparticles present a distribution, hemispherical shape and average diameter similar to

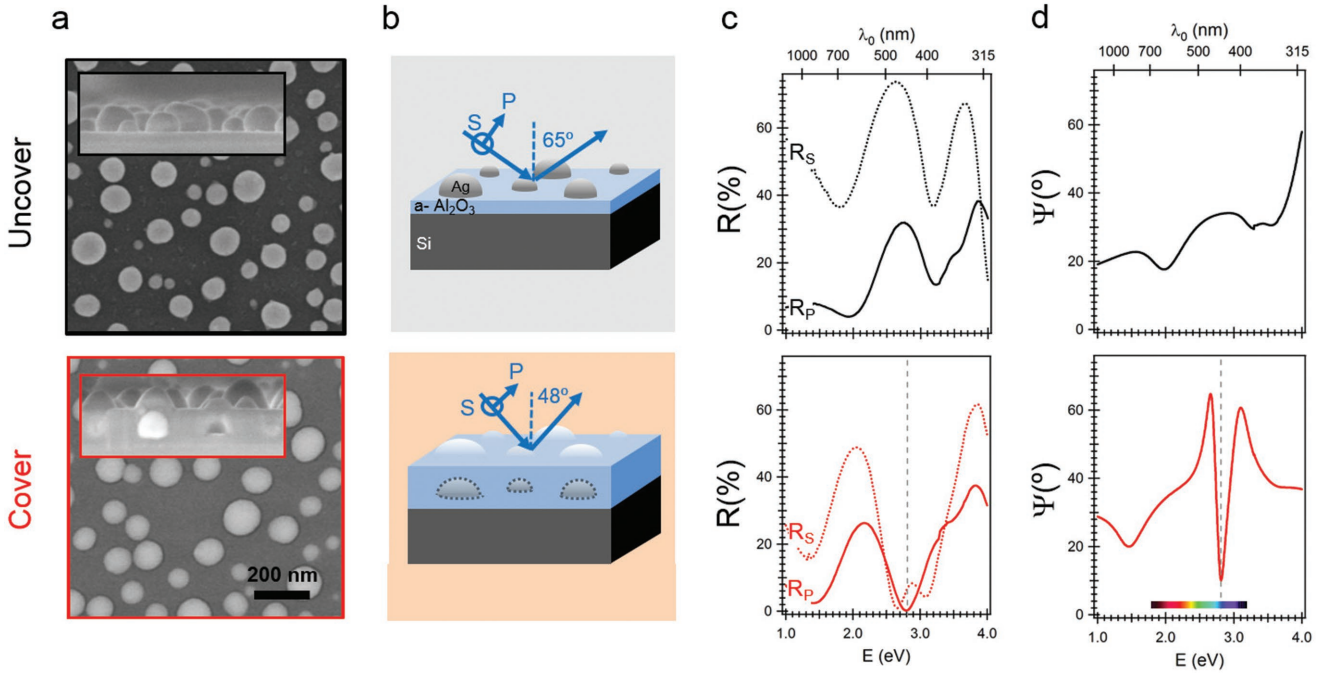

Figure 1. Nanostructure and room-temperature optical properties of the "uncover" and "cover" metasurfaces. a) Scanning electron images: top-view and cross-section (insets). b) Configuration of the optical measurements. The orientation of the electric field for s- and p-polarized incident light is denoted as "s" and "p," respectively. c) Room-temperature specular reflectance spectra for s- and p-polarized light, R_s and R_p, respectively, for an angle of incidence (AOI) of 65° ("uncover" metasurface) and 48° ("cover" metasurface). d) Room-temperature spectra of the ellipsometric amplitude coefficient Ψ at the same AOIs. The "cover" metasurface shows a sharp drop and near cancelation of Ψ for (AOI = 48°, photon energy $E \approx 2.8$ eV) where quasi-darkness conditions are fulfilled.

those of the "uncover" metasurface. However, in this case, the nanoparticles are fully buried below the a-Al_2O_3 cover layer, whose topography replicates conformally the morphology and distribution of the nanoparticles underneath. The top of the "cover" metasurface thus consists of an amorphous 2D array of nanodomes on a flat background (Section S1, Supporting Information).

The optical properties in the ultraviolet, visible, and near infrared of the "uncover" and "cover" metasurfaces were first characterized by specular reflectance spectroscopy with s- and p-polarized light, in a broad range of angles of incidence (AOI from 20° to 70°), at room temperature. The measurement configuration is depicted in Figure 1b, and the setup is described in Section S2 of the Supporting Information. For the "cover" metasurface (Figure 1c (bottom panel)), the p-polarized reflectance R_p presents a marked minimum with a near-zero value ($R_p^{min} \approx 0.25°$) at the AOI of 48° for a photon energy $E \approx 2.8$ eV. This response is characteristic of quasi-darkness conditions, where the p-polarized beam is very weakly reflected by the metasurface. No such conditions could be observed at any AOI and polarization (s or p) for the "uncover" metasurface. This can be seen from Figure 1c (top panel) that shows the reflectance spectra of this structure at the AOI of 65°, at which its most pronounced minima were observed for R_p. These minima are not marked enough ($R_p^{min} \approx 4°$ and 14°) to allow quasi-darkness conditions to be fulfilled.

Spectroscopic ellipsometry measurements in the ultraviolet, visible, and near infrared were then performed on the two kinds of metasurfaces to determine the amplitude and phase of the reflected light, at room temperature. Details about the measurement setup are given in Section S2 of the Supporting Information. Figure 1d shows the spectra of the ellipsometric amplitude coefficient Ψ of the "uncover" (top panel) and "cover" (bottom panel) metasurfaces. This coefficient represents the $|r_p/r_s|$ ratio, r_p and r_s being the Fresnel reflection coefficients of the metasurface, which relate with reflectance following the relations: $R_p = |r_p|^2$; $R_s = |r_s|^2$. Therefore, quasi-darkness conditions for p-polarized light ($R_p \to 0$) translate into a sharp minimum and a near cancelation of Ψ as observed for the "cover" metasurface for AOI = 48° and $E \approx 2.8$ eV. No other sharp minimum of Ψ could be observed in the studied spectral range for this metasurface, even by varying the AOI (Section S2, Figure S2.1, Supporting Information). Note however that sharp Ψ maxima are observed at (AOI = 60°, $E \approx 2.65$ eV) and (AOI = 70°, $E \approx 3.2$ eV), due to the near-zero value of R_s in these conditions for which the "cover" metasurface presents quasi-darkness for s-polarized light. As no such near-zero values of neither R_s nor R_p are achieved at any AOI for the "uncover" metasurface, its Ψ spectra depend weakly on photon energy (Section S2, Figure S2.2, Supporting Information).

The spectrum of the ellipsometric phase coefficient Δ of the "cover" metasurface for an AOI of 48° is shown in **Figure 2**a (bottom panel). This coefficient represents the phase shift between the p- and s-polarized components of light induced by reflection. At $E = 2.8$ eV where quasi-darkness conditions are fulfilled for p-polarized light ($R_p \to 0$ and $\Psi \to 0$), Δ turns abruptly by 170°, from 260° to 90°. This behavior originates from a jump in the phase of the near-zero-intensity p-polarized reflected light.[37] Note that additional abrupt Δ variations can be seen at the AOIs and photon energies of the sharp Ψ maxima where $R_s \to 0$ (Section S2, Figure S2.1, Supporting Information). In that case, such variations originate from jumps in the phase of the near-zero-intensity s-polarized reflected light.

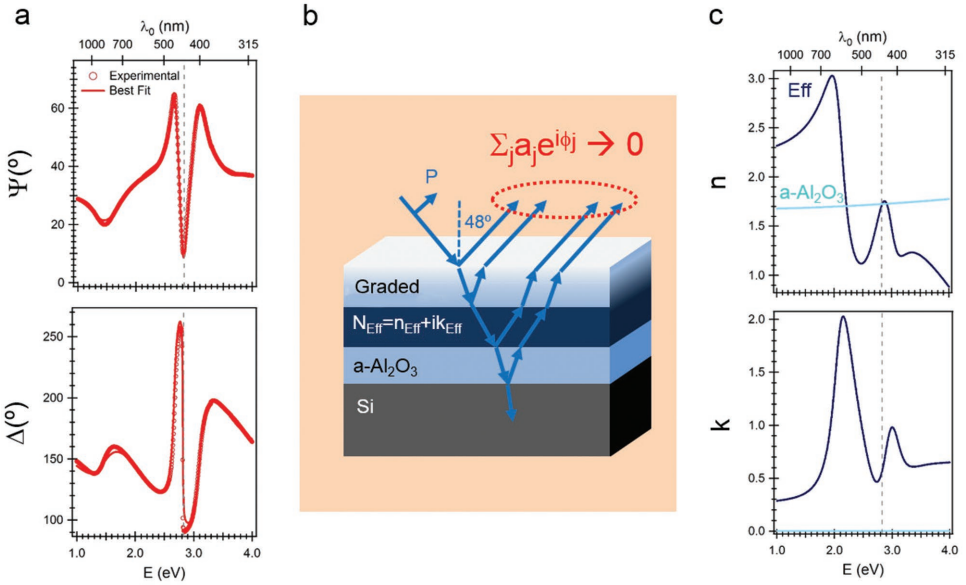

Figure 2. "Cover" metasurface: reflected light phase jump in quasi-darkness conditions enabled by thin film interference–plasmon resonances hybridization. a) Experimental and best-fit simulated room-temperature spectra of the ellipsometric amplitude and phase coefficients, Ψ and Δ, for an AOI of 48°. An abrupt Δ variation occurs in the quasi-darkness conditions (AOI = 48°, $E \approx 2.8$ eV). b) Equivalent model (layered structure) used for simulating the ellipsometry spectra. The buried Ag nanoparticles layer is represented by an effective medium with complex refractive index $N_{eff} = n_{eff} + ik_{eff}$. c) Best-fit spectra of n_{eff} and k_{eff} together with the n and k of a-Al_2O_3. The vertical dashed line points at $E \approx 2.8$ eV where the quasi-darkness conditions are fulfilled (for an AOI of 48°). The specific values of n_{eff} and k_{eff} at this E value allow almost fully destructive interferences for the p-polarized reflected light, as depicted in red in (b).

To elucidate the origin of the quasi-darkness conditions and related phase jump in the "cover" metasurface, we modeled it as a layered structure (Figure 2b) in which the buried Ag nanoparticles layer is represented by an effective medium and the conformal a-Al_2O_3 cover layer is represented by a graded medium. More details about the model and simulations are given in Section S3 of the Supporting Information. In particular, we show in Section S3 of the Supporting Information that the effective medium approach is suitable for fitting the experimental Ψ, Δ, R_p, and R_s spectra of the "cover" metasurface in a broad range of AOIs, from 20° to 70°. This supports the validity of the proposed effective medium-based modeling for describing the macroscopic optical properties of this specific metasurface that are concerned in the sensing experiment, and for providing an equivalent model capturing its relevant physical features and describing its sensing performance. From numerical fitting of the experimental Ψ and Δ spectra, the effective refractive index n_{eff} and extinction coefficient k_{eff} of the buried Ag nanoparticles layer were determined. Their spectra, shown in Figure 2c, are dominated by two resonances, peaking near 2.2 and 2.9 eV, in good qualitative agreement with the transmittance spectrum of a similar "cover" metasurface grown on a transparent fused silica substrate (Section S4, Supporting Information). Both resonances are also seen in the transmittance spectrum of an "uncover" metasurface on fused silica, where they nevertheless peak at higher photon energies (Section S4, Supporting Information). These environment-sensitive resonances are attributed to the localized surface plasmon resonance modes of the Ag nanoparticles: dipolar and quadrupolar modes near 2.2 and 2.9 eV, respectively. For the "cover" metasurface, these resonances enable n_{eff} and k_{eff} values suitable for achieving almost fully destructive interference for p-polarized light in the layered structure at a specific AOI (48°) and photon energy ($E \approx 2.8$ eV) (Figure 2b; Section S5, Supporting Information). Therefore, the quasi-darkness conditions of the "cover" metasurface, and thus the related phase jump, can be described with an equivalent model in which the interplay between thin film interference and localized surface plasmon resonances confers them a hybrid origin. Such equivalent model of the "cover" metasurface reflects the photonic-plasmonic design of this metasurface. According to this model, the magnitude and photon energy of the plasmon resonances are primarily defined by the Ag nanoparticles size, shape, 2D organization and environment, and the tuning of the vertical layered structure enables the necessary phase shifts to achieve fully destructive interference at the required photon energies and AOIs. Thus, it is important to note the key role of the a-Al_2O_3 cover layer in the design of the metasurface: according to the proposed equivalent model, the absence of an a-Al_2O_3 cover layer limits the optical path in the layered structure, in which the accumulated phase shifts are insufficient to achieve fully destructive interference at any AOI. This simple theoretical consideration is validated by the fact that no quasi-darkness and phase jumps are observed for the "uncover" metasurface (Figure S2.2, Supporting Information), thus further showing the capability of the proposed equivalent model to capture the relevant physical features of the studied metasurfaces.

Here, we show the suitability of the "cover" metasurface as temperature-sensitive platform for optical thermometry, by monitoring the phase of the reflected p-polarized light in quasi-darkness conditions. To demonstrate this property, the Δ spectrum of this metasurface was measured by spectroscopic ellipsometry as a function of temperature in the 25–55 °C range, for an AOI of 48°. **Figure 3**a shows the measured spectra in the region near the phase jump, at selected temperatures. Upon temperature increase from 25 to 45 °C, Δ varies gradually in a narrow spectral region (2.806–2.808 eV, or 441.5–441.2 nm) where a 180° change is finally achieved. Upon increasing temperature to 55 °C, the Δ jump flips completely. Furthermore, as shown in Figure 3b, the specular reflectance R_p and R_s values of the metasurface remain unchanged upon varying temperature in the range considered here. Thus, probing the phase of the reflected light in the spectral region of the jump allows the monitoring of temperature with a much higher resolution than with traditional specular reflectance measurements.

To estimate the achievable resolution with such optical thermometry scheme, the ellipsometric phase coefficient Δ has been plotted as a function of temperature, at a selected photon energy ($E = 2.807$ eV, Figure 3c). At this photon energy, the $\Delta = f$ (temperature) curve shows a maximum slope at the low temperature side of the graph (25 °C). A linear fitting in this region yields a slope of 15° in Δ per 1 °C in temperature. Thus, with a 0.1° resolution in the Δ measurement, the temperature will be determined with a 7×10^{-3} °C resolution. With a 0.01° resolution in the Δ measurement (standard limit in ellipsometry experiments), temperature can be determined with a 7×10^{-4} °C resolution. Note that because the Δ measurements are performed in quasi-darkness conditions, the measured optical signals present a very low intensity. Therefore, reaching the temperature resolutions given above requires to maximize the signal-to-noise ratio in the measurement of Δ (by realizing, for instance, noise filtering, averaging, measurement at different photon energies and spectral fitting). By plotting $\Delta = f$ (temperature) at a different photon energy (Section S6, Figure S6.2, Supporting Information), the temperature range of optimum resolution can be shifted to higher temperatures. Therefore, it is possible to achieve optical thermometry with high resolution in a relatively broad temperature range by simply monitoring the phase of the reflected light at a different photon energy. To further evaluate the potential of the "cover" metasurface for optical thermometry, its stability versus heating–cooling cycles was tested, showing a good reversibility upon cycling between 25 and 55 °C. The proof of such reversibility is shown in Section S6, Figure S6.3 of the Supporting Information, where it is shown that the final Δ spectrum of the metasurface after 25 °C → 55 °C → 25 °C heating–cooling is identical to the initial one. Such reversibility is likely favorized by the stability and robustness of the a-Al_2O_3 cover layer, which is very efficient in blocking the temperature-induced reshaping of metal nanoparticles, their chemical degradation, and material exodiffusion.[45,46] To demonstrate the temperature sensitivity of a "cover" metasurface in a real experiment; we studied the evolution of its Δ upon laser heating, where a continuous laser beam was shined onto the metasurface. The results of such experiment are shown in Figure 3d. Upon turning on the laser beam, the Δ jump shifts toward a smaller photon energy, as a result of the laser-induced temperature increase. After

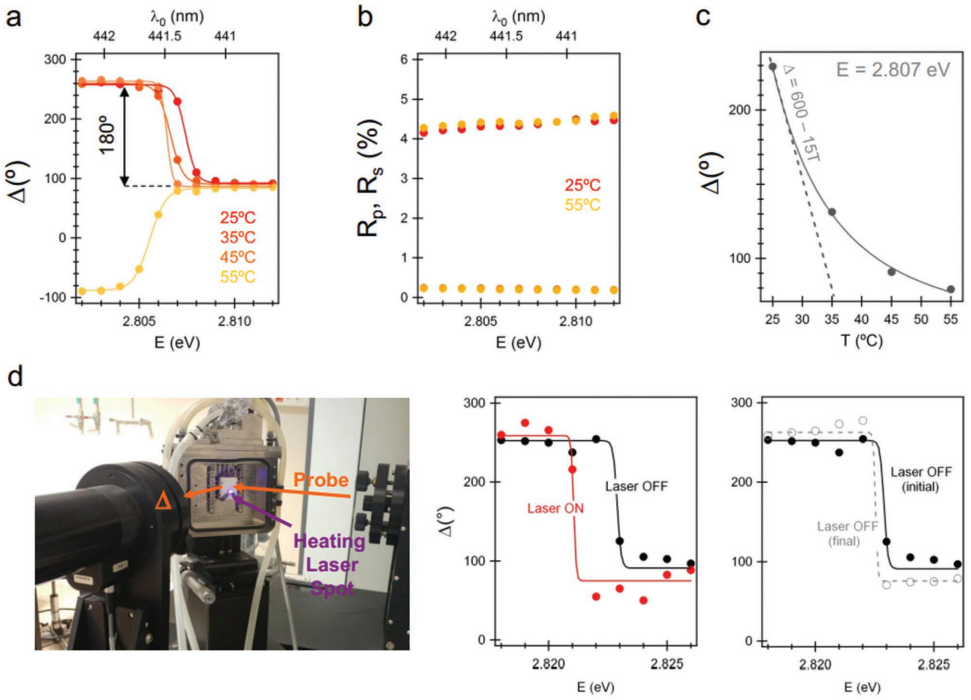

Figure 3. Optical thermometry by monitoring the phase of the reflected light in quasi-darkness conditions. a) Spectrum of the ellipsometric coefficient Δ of the "cover" metasurface (AOI = 48°) at different temperatures from 25 to 55 °C. b) Specular reflectance spectra for s- polarized and p-polarized light (R_s and R_p) of the same metasurface at 25 and 55 °C. c) Variation of the ellipsometric coefficient Δ at a photon energy of 2.807 eV as a function of temperature. The dashed line is a linear fit of the low temperature part of the graph, yielding the responsivity of the optical thermometry scheme: 15° in Δ per °C in temperature. d) Optical thermometry during laser heating of a "cover" metasurface: picture of the experimental setup (left), spectrum of the ellipsometric coefficient Δ before shining the laser versus with the laser on (middle), and before shining the laser and after turning it off (right). This shows the suitability of the metasurface for monitoring optically laser-induced heating, and the reversibility of the measurement scheme.

turning off the laser, the Δ jump comes back to its initial position. This points again at the good reversibility of the "cover" metasurface.

Summarizing, we have unveiled a nondemanding photonic-plasmonic metasurface design suitable for being used as temperature-sensitive platform for high-resolution optical thermometry. It is much easier to implement than previously reported photonic-plasmonic architectures that combined plasmonic nanostructures with microresonators or photonic structures to achieve highly environment-sensitive hybrid resonances with high quality factor and small mode volume.[47–51] The on-chip implementation of such structures required using lithography techniques or building periodic multilayers thicker than the wavelength of light. Such fabrication routes are also needed for the implementation of microresonators,[1–8] microinterferometers,[9,10] or Tamm plasmonic structures,[17,44] respectively. Here, the metasurface structure is compatible with a lithography-free two-layer fabrication process, affordable either by physical deposition or solution-processing. Because the size/shape/distance distribution of the Ag nanoparticles in the metasurface is dictated only by the initial Ag layer thickness and the Ag annealing temperature and atmosphere, which can be very accurately controlled together with the a-Al_2O_3 layer thicknesses during the pulsed laser deposition process (where thickness accuracy is less than 1 nm), a good reproducibility can be achieved for the macroscopic optical properties of the metasurface that are probed during the sensing experiments. For instance, we estimate that, at best, a 10 nm reproducibility can be achieved for the plasmon resonance wavelength. Let us note that the proof-of-concept metasurface we show is simple and thus at reach of other well established self-assembly fabrication techniques.

The high sensing resolution enabled by such nondemanding design originates from the hybridization of two low-quality-factor phenomena, thin film interference and localized surface plasmon resonances, which yields quasi-darkness conditions where a sharp spectral variation ("a jump") of the phase of light reflected by the metasurface occurs. This jump is equivalent, for sensing purposes, with a high-quality-factor resonator showing a strong sensitivity to temperature. By monitoring the phase of light reflected by the temperature-sensitive metasurface in such quasi-darkness conditions, a temperature resolution below the 10^{-3} °C range can be reached. This high resolution can be achieved in a broad range of temperature upon tuning the probe photon energy.

Finally, it is important that these high-resolution optical thermometry measurements have been realized in a standard optical reflectance configuration with no need of special light in-coupling or out-coupling strategies or structures (Section S2, Supporting Information). Furthermore, the measurements were done using a lamp by selecting a relatively broad light bandwidth (8 nm, Section S2, Supporting Information). Therefore, in contrast with microresonators or microinterferometers, neither a high light intensity, nor a highly monochromatic laser

source is required for the proposed sensing scheme. Indeed, the spectral bandwidth does not affect strongly the phase jump (Section S7, Supporting Information), and in fact it can be set as fixed parameter during the sensing experiment. This provides an advantage for the proposed sensing scheme versus other approaches based on active sensing systems, such as luminescence nanothermometry. Such approaches, which have shown excellent temperature resolutions (they enable reaching the range of 10^{-3} °C),[52,53] however usually require the use of laser sources to induce luminescence signals with enough intensity.

As a conclusion, this work shows how an easily built photonic-plasmonic metasurface design is suitable to enable high-resolution optical thermometry with an easy-to-implement measurement scheme. This points at its powerful potential as a practical alternative to microresonators and microinterferometers for optical thermometry. Furthermore, the concept discussed here can be applied to a broader range of materials (beyond noble metals and common dielectrics) to enable higher temperature resolutions in ultrathin metasurfaces.

Experimental Section

The metasurfaces were fabricated by pulsed laser deposition in a vacuum chamber, where Ag and Al_2O_3 targets were ablated sequentially. The setup is described in detail in ref. [45] and references therein. The annealing at 350 °C of the Ag coating was done in air. The specular reflectance and spectroscopic ellipsometry measurements were done with a VASE ellipsometer (Woollam Co. Inc.); more details about these measurements and the setup configurations are given in Section S2 of the Supporting Information. The temperature-dependent ellipsometry measurements were done with the same setup, equipped with an Instec heat stage. These measurements were done in real-time: the ellipsometric response of the metasurface was measured versus time, while temperature was varied by steps in a controlled way using the heating stage. The laser heating experiments were done by shining a continuous violet laser light (Ekspla, 13 mW, 409 nm) at near-normal incidence on the "cover" metasurface. The ellipsometric response was measured prior to shining the laser, with the laser on and then with the laser off again, each time after waiting that the metasurface temperature was stabilized. In all the temperature-dependent experiments, which were performed in quasi-darkness conditions where the reflected light intensity is very low, acquisition times of ≈20 s were used for the measurement of Δ at each photon energy. The optical data analysis and simulations were done with the WVASE32 software (Woollam Co. Inc.); more details are given in Section S3 of the Supporting Information.

Supporting Information

Supporting Information is available from the Wiley Online Library or from the author.

Acknowledgements

The authors are grateful to Thomas Wagner (Lot Oriel Co.) for advice during the data analysis. M.G.P. acknowledges support from the European Social Fund and G.B. a CSIC-JAE predoctoral grant, cofunded by the European Social Fund. This work was funded in part by the Spanish Ministry for Economy and Competitiveness through the project MINECO/FEDER TEC2015-69916-C2-1-R. G.B. fabricated the metasurfaces and coordinated the structural characterization under the supervision of J.G. and performed the optical measurements at room temperature; M.G.P. performed the optical measurements as a function of temperature under the supervision of R.S., who designed the experiment; J.T. proposed the concept, performed the optical modeling, fitting, and analysis, and wrote the paper with the input from all the authors.

Conflict of Interest

The authors declare no conflict of interest.

Keywords

metasurfaces, optical phase, plasmon, remote sensing, self-assembly

Received: February 9, 2018
Revised: March 18, 2018
Published online: May 2, 2018

[1] K. D. Heylman, K. A. Knapper, E. H. Horak, M. T. Rea, S. K. Vanga, R. H. Goldsmith, *Adv. Mater.* **2017**, *29*, 1700037.
[2] K. D. Heylman, N. Thakkar, E. H. Horak, S. C. Quillin, C. Cherqui, K. A. Knapper, D. J. Masiello, R. H. Goldsmith, *Nat. Photonics* **2016**, *10*, 788.
[3] H.-T. Kim, M. Yu, *Opt. Express* **2016**, *24*, 9501.
[4] L. Stern, A. Naiman, G. Keinan, N. Mzurski, M. Grajower, U. Levy, *Optica* **2017**, *4*, 1.
[5] L. Wan, H. Chandrahalim, C. Chen, Q. Chen, T. Mei, Y. Oki, N. Nishimura, L.-J. Guo, X. Fan, *Appl. Phys. Lett.* **2017**, *111*, 061109.
[6] W. Weng, J. D. Anstie, A. N. Luiten, *Phys. Rev. Appl.* **2015**, *3*, 044015.
[7] C.-H. Dong, L. He, Y.-F. Xiao, V. R. Gaddam, S. K. Ozdemir, Z.-F. Han, G.-C. Guo, L. Yang, *Appl. Phys. Lett.* **2009**, *94*, 231119.
[8] L. Xu, X. Jiang, G. Zhao, D. Ma, H. Tao, Z. Liu, F. G. Omenetto, L. Yang, *Opt. Express* **2016**, *24*, 20825.
[9] J.-F. Tao, H. Cai, Y.-D. Gu, J. Wu, A.-Q. Lu, *IEEE Photonics Technol. Lett.* **2015**, *27*, 767.
[10] X. Guan, X. Wang, L. H. Frandsen, *Opt. Express* **2016**, *24*, 16349.
[11] C. Langhammer, E. M. Larsson, B. Kasemo, I. Zoric, *Nano Lett.* **2010**, *10*, 3629.
[12] H. Reddy, U. Guler, K. Chaudhuri, A. Dutta, A. V. Kildishev, V. M. Shalaev, A. Boltasseva, *ACS Photonics* **2017**, *4*, 1083.
[13] L. J. Davis, M. Deutsch, *Rev. Sci. Instrum.* **2010**, *81*, 114905.
[14] S. K. Özdemir, *J. Lightwave Technol.* **2003**, *21*, 805.
[15] H.-P. Chiang, H.-T. Yeh, C.-M. Chen, J.-C. Wu, S.-Y. Su, R. Chang, Y.-J. Wu, D.-P. Tsai, S.-U. Jen, P.-T. Leung, *Opt. Commun.* **2004**, *241*, 409.
[16] N. Hirayama, Y. Sano, *ISA Trans.* **2000**, *39*, 169.
[17] P. S. Maji, R. Das, *J. Lightwave Technol.* **2017**, *35*, 2833.
[18] N. Yu, F. Capasso, *Nat. Mater.* **2014**, *13*, 139.
[19] A. Y. Zhu, A. I. Kuznetsov, B. Luk'Yanchuk, N. Engheta, P. Genevet, *Nanophotonics* **2017**, *6*, 2.
[20] A. M. Urbas, Z. Jacob, L. Dal Negro, N. Engheta, A. D. Boardman, P. Egan, A. B. Khanikaev, V. Menon, M. Ferrera, N. Kinsey, C. DeVault, J. Kim, V. Shalaev, A. Boltasseva, J. Valentine, C. Pfeiffer, A. Grbic, E. Narimanov, L. Zhu, S. Fan, A. Alù, E. Poutrina, N. M. Litchinitser, M. A. Noginov, K. F. MacDonald, E. Plum, X. Liu, P. F. Nealey, C. R. Kagan, C. B. Murray, D. A. Pawlak, I. I. Smolyaninov, V. N. Smolyaninova, D. Chanda, *J. Optom.* **2016**, *18*, 9.
[21] H. Mühlenbernd, P. Georgi, N. Pholchai, L. Huang, G. Li, S. Zhang, T. Zentgraf, *ACS Photonics* **2016**, *3*, 124.

[22] A. Karvounis, B. Gholipour, K. F. MacDonald, N. I. Zheludev, *Appl. Phys. Lett.* **2016**, *109*, 051103.
[23] W. Lewandowski, M. Fruhnert, J. Mieckzkowski, C. Rockstuhl, E. Górecka, *Nat. Commun.* **2015**, *6*, 6590.
[24] T. Lewi, H. A. Evans, N. A. Butakov, J. A. Schuller, *Nano Lett.* **2017**, *17*, 3940.
[25] G. Garcia, R. Buonsanti, A. Llordes, E. L. Runnerstrom, A. Bergerud, D. J. Milliron, *Adv. Opt. Mater.* **2013**, *1*, 215.
[26] J. Park, J.-H. Kang, S. J. Kim, X. Liu, M. L. Brongersma, *Nano Lett.* **2017**, *17*, 407.
[27] Z. Zhu, P. G. Evans, R. F. Haglund Jr., J. G. Valentine, *Nano Lett.* **2017**, *17*, 4881.
[28] A. Woessner, Y. Gao, I. Torre, M. B. Lundeberg, C. Tan, K. Watanabe, T. Taniguchi, R. Hillenbrand, J. Hone, M. Polini, F. H. L. Koppens, *Nat. Photonics* **2017**, *11*, 421.
[29] M. C. Sherrott, P. W. Hon, K. T. Fountaine, J. C. Garcia, S. M. Ponti, V. W. Brar, L. A. Sweatlock, H. A. Atwater, *Nano Lett.* **2017**, *17*, 3027.
[30] K. Thyagarajan, R. Sokhoyan, L. Zornberg, H. A. Atwater, *Adv. Mater.* **2017**, *29*, 1701044.
[31] Y.-W. Huang, H. W. H. Lee, R. Sokhoyan, R. A. Pala, K. Thyagarajan, S. Han, D. P. Tsai, H. A. Atwater, *Nano Lett.* **2016**, *16*, 5319.
[32] R. Yu, V. Pruneri, F. J. Garcia de Abajo, *Sci. Rep.* **2016**, *6*, 32144.
[33] R. F. Waters, P. A. Hobson, K. F. MacDonald, N. I. Zheludev, *Appl. Phys. Lett.* **2015**, *107*, 081102.
[34] Y. Yang, K. Kelley, E. Sachet, S. Campione, T. S. Luk, J.-P. Maria, M. B. Sinclair, I. Brener, *Nat. Photonics* **2017**, *11*, 390.
[35] M. Clerici, N. Kinsey, C. DeVault, J. Kim, E. G. Carnemolla, L. Caspani, A. Shaltout, D. Faccio, V. Shalaev, A. Boltasseva, M. Ferrera, *Nat. Commun.* **2017**, *8*, 15829.
[36] V. G. Kravets, F. Schedin, R. Jalil, L. Britnell, R. V. Gorbachev, D. Ansell, B. Thackray, K. S. Novoselov, A. K. Geim, A. V. Kabashin, A. N. Grigorenko, *Nat. Mater.* **2013**, *12*, 304.
[37] M. Svedendahl, R. Verre, M. Käll, *Light: Sci. Appl.* **2014**, *3*, e220.
[38] H. Song, N. Zhang, J. Duan, Z. Liu, J. Gao, M. H. Singer, D. Ji, A. R. Cheney, X. Zeng, B. Chen, S. Jiang, Q. Gan, *Adv. Opt. Mater.* **2017**, *5*, 1700166.
[39] R. Paniagua-Domínguez, Y. F. Yu, A. E. Miroshnichenko, L. A. Krivitsky, Y. H. Fu, V. Valuckas, L. Gonzaga, Y. T. Toh, A. Y. S. Kay, B. Luk'yanchuk, A. I. Kuznetsov, *Nat. Commun.* **2016**, *7*, 10362.
[40] J. Toudert, X. Wang, C. Tallet, P. Barois, A. Aradian, V. Ponsinet, *ACS Photonics* **2015**, *2*, 1443.
[41] A. I. Aristov, M. Manousidaki, A. Danilov, K. Terzaki, C. Fotakis, M. Farsari, A. V. Kabashin, *Sci. Rep.* **2016**, *6*, 25380.
[42] L. Malassis, P. Massé, M. Tréguer-Delapierre, S. Mornet, P. Weisbecker, P. Barois, C. R. Simovski, V. G. Kravets, A. N. Grigorenko, *Adv. Mater.* **2014**, *26*, 324.
[43] A. N. Grigorenko, P. I. Nikitin, A. V. Kabashin, *Appl. Phys. Lett.* **1999**, *75*, 3917.
[44] Y. Tsurimaki, J. K. Tong, V. N. Boriskin, A. Semenov, M. I. Ayzatsky, Y. P. Machekhin, G. Chen, S. Boriskina, *ACS Photonics* **2018**, *5*, 929.
[45] G. Baraldi, M. Carrada, J. Toudert, F. J. Ferrer, A. Arbouet, V. Paillard, J. Gonzalo, *J. Phys. Chem. C* **2013**, *117*, 9431.
[46] J. Toudert, R. Serna, M. Jiménez de Castro, *J. Phys. Chem. C* **2012**, *116*, 20530.
[47] W. Ahn, S. V. Boriskina, Y. Hing, B. M. Reinhard, *ACS Nano* **2012**, *6*, 951.
[48] M. Barth, S. Schietinger, S. Fischer, J. Becker, N. Nüsse, T. Aichele, B. Löchel, C. Sönnichsen, O. Benson, *Nano Lett.* **2010**, *10*, 891.
[49] V. R. Dantham, S. Holler, C. Barbre, D. Keng, V. Kolchenko, S. Arnold, *Nano Lett.* **2013**, *13*, 3347.
[50] Y. Luo, M. Chamanzar, A. Apuzzo, R. Salas-Montiel, K. Ngoc Nguyen, S. Blaize, A. Adibi, *Nano Lett.* **2015**, *15*, 849.
[51] X. Wang, R. Morea, J. Gonzalo, B. Palpant, *Nano Lett.* **2015**, *15*, 2633.
[52] D. Jaque, F. Vetrone, *Nanoscale* **2012**, *4*, 4301.
[53] S. S. Laha, A. R. Naik, E. R. Kuhn, M. Alvarez, A. Sujkowski, R. J. Wessells, B. P. Jena, *Nano Lett.* **2017**, *17*, 1262.